ISSN 0021-3640, JETP Letters, 2021, Vol. 113, No. 1, pp. 57–60. © Pleiades Publishing, Inc., 2021.
Russian Text © The Author(s), 2021, published in Pis'ma v Zhurnal Eksperimental'noi i Teoreticheskoi Fiziki, 2021, Vol. 113, No. 1, pp. 63–67.

CONDENSED MATTER

# Band Structure of Tungsten Oxide $W_{20}O_{58}$ with Ideal Octahedra

**M. M. Korshunov[a, *], I. A. Nekrasov[b], N. S. Pavlov[b], and A. A. Slobodchikov[b, **]**

[a] *Kirensky Institute of Physics, Federal Research Center KSC, Siberian Branch, Russian Academy of Sciences, Akademgorodok, Krasnoyarsk, 660036 Russia*

[b] *Institute of Electrophysics, Ural Branch, Russian Academy of Sciences, Yekaterinburg, 620016 Russia*

**e-mail: mkor@iph.krasn.ru*

***e-mail: slobodchikov@iep.uran.ru*

Received November 24, 2020; revised November 25, 2020; accepted November 25, 2020

The band structure, density of states, and the Fermi surface of a tungsten oxide $WO_{2.9}$ with idealized crystal structure (ideal octahedra $WO_6$ creating a "square lattice") is obtained within the density functional theory in the generalized gradient approximation. Because of the oxygen vacancies ordering this system is equivalent to the compound $W_{20}O_{58}$ (Magnéli phase), which has 78 atoms in unit cell. We show that 5*d*-orbitals of tungsten atoms located immediately around the voids in the zigzag chains of edge-sharing octahedra give the dominant contribution near the Fermi level. These particular tungsten atoms are responsible of low-energy properties of the system.

**DOI:** 10.1134/S0021364021010057

## 1. INTRODUCTION

Superconductivity, as one of the fundamental ground states in solid state physics, is realized sometimes in the most unexpected cases. These are both high-temperature superconducting cuprates [1], which are dielectrics in the underdoped case, as well as pnictides and iron chalcogenides [2–5], although under normal conditions iron is a ferromagnet. These systems are unusual superconductors, i.e., having an anisotropic momentum dependence of the order parameter. They are related to tungsten oxides by the presence of a partially filled *d*-shell. Oxygen non-stoichiometric $WO_{3-x}$ tungsten trioxide compounds have been known for a long time and their structure and properties have been well studied [6, 7]. However, more recently, the discovery of superconductivity in the compound $WO_{2.9}$ with $T_c = 80$ K and with $T_c = 94$ K when intercalated with lithium [8] has been reported. This was preceded by the observation of superconductivity near the domain walls in $WO_{3-x}$ [9], thin films [10] and in $WO_3$ with surface deposited sodium, $Na_{0.05}WO_3$ [11], which led to the prediction of the possibility of superconductivity realization in $WO_{3-x}$ [12].

Despite the long history of research on tungsten oxides, there are only a few works on the band structure calculations of $WO_3$. These are works on the electronic structure of bulk samples, thin films and clusters [13–20], the role of oxygen vacancies [21–25] and cationic doping [26–33]. Calculations for Magnéli phases with ordered oxygen vacancies, $WO_{3-x}$, are described in only one work [34], which illustrate that the compounds $W_{32}O_{84}$, $W_3O_8$, $W_{18}O_{49}$, $W_{17}O_{47}$, $W_5O_{14}$, $W_{20}O_{58}$, and $W_{25}O_{73}$ show metallic properties.

The ordering of oxygen vacancies in the system $WO_{3-x}$ leads to the appearance of quite large unit cells, which significantly complicates its description. In addition, superconductivity is realized in the system $W_{20}O_{58}$ containing 78 atoms in a unit cell. Tungsten atoms coordinated by oxygen atoms form octahedra, which are either corner sharing or edge sharing. The octahedra themselves are distorted, and the W–O–W bonds between the octahedra are distorted as well, which leads to an additional complication of the description of the electronic structure of $W_{20}O_{58}$.

Since the foundation for building a superconducting state theory is the band structure of the normal phase, the calculation of the last one from the first principles will be the first step on this path. In this work, we obtained the band structure, density of states, and Fermi surface for the compound $WO_{3-x}$ with ideal octahedra creating a square lattice, which is the first approximation in the description of this complex compound.

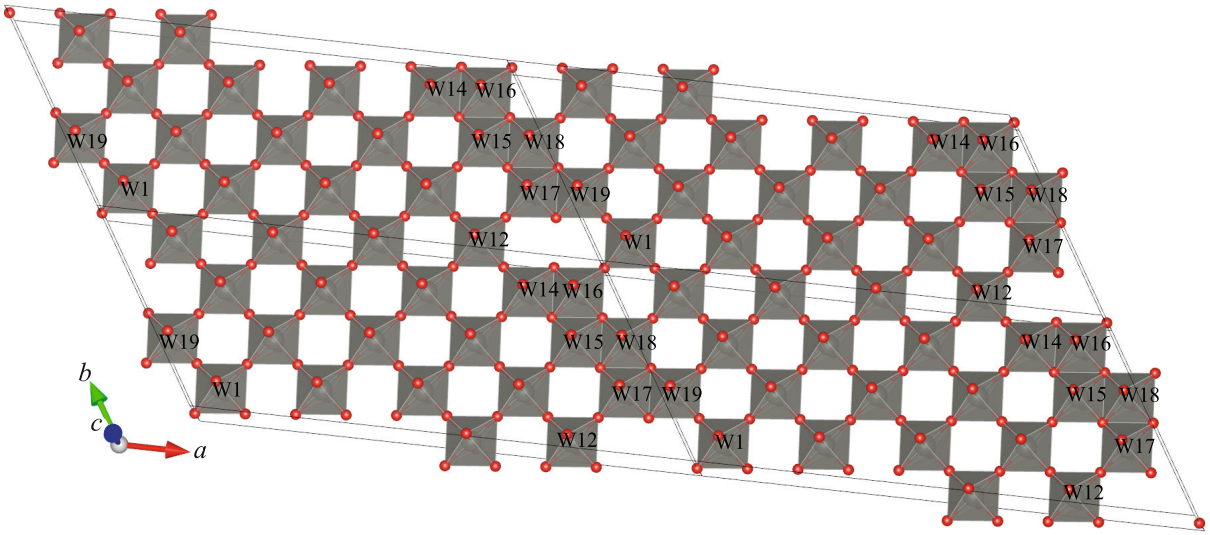


**Fig. 1.** (Color online) Idealized crystal structure of the $W_{20}O_{58}$ supercell (2 × 2 × 1).

## 2. STRUCTURE AND CALCULATION RESULTS

$W_{20}O_{58}$ belongs to the family of oxides with the Magnéli structure and the general formula $W_nO_{3n-2}$ [6]. Space group is $P2/m{:}b$, lattice parameters are $a = 23.39$ Å, $b = 12.1$ Å, $c = 3.78$ Å, $\gamma = 95°$ [35]. The crystal structure consists of $WO_6$ octahedra which are either corner sharing or edge sharing in the (100) plane.

As stated earlier in the compound $W_{20}O_{58}$ the $WO_6$ octahedra are distorted and the O–O bond length ranges from 2.63 to 2.72 Å. In order to model the idealized crystal structure, all octahedra were made ideal with average oxygen–oxygen distance equal to 2.68 Å. In this case, the bases of all ideal octahedra form a square lattice. Figure 1 shows the 2 × 2 × 1 supercell for the idealized crystal structure $W_{20}O_{58}$.

To calculate the band structure, the density of states (DOS) and the Fermi surface we use the density functional theory (DFT) with all-electron full-potential linearized augmented-plane wave method (FP-LAPW) implemented via the Elk code [37] together with the generalized gradient approximation (GGA) [36]. For the self-consistent ground state calculation, we used a 8 × 8 × 8 **k**-points grid in an irreducible Brillouin zone making sure that the results are almost indistinguishable from those for a 6 × 6 × 6 grid.

The density of states in the wide energy range is shown in Fig. 2. The top of the valence band from –0.8 to –4.0 eV is formed mainly by O-2*p* states. In the region from –4.0 to –9.0 eV, we see strong hybridization of W-5*d* and O-2*p* states.

In the stoichiometric compound $WO_3$, tungsten $W^{6+}$ has a $5d^0$ configuration, that is, an empty 5*d*-shell and, therefore, a completely filled O-2*p* shell, being a band dielectric. The oxygen deficit in $WO_{3-x}$ leads to electron doping and a finite conductivity value [7]. This is clearly seen in our calculation as well, where the W-5*d* states are almost empty and form the conduction band. At the Fermi level, we can see only

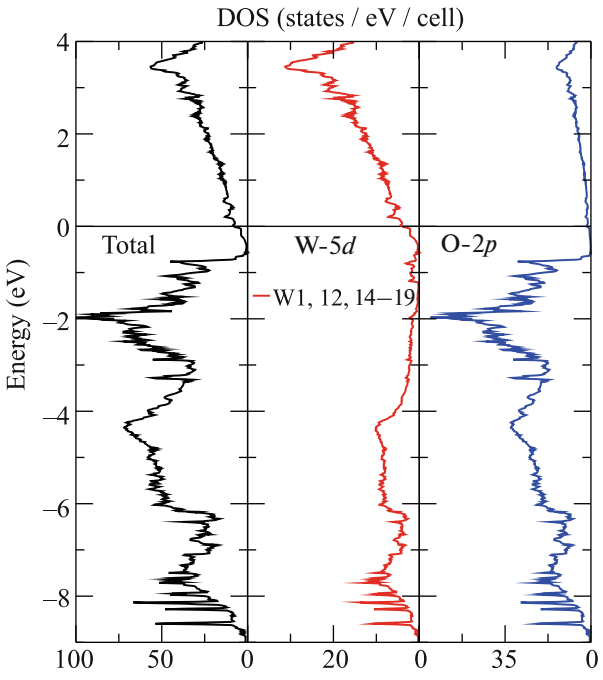


**Fig. 2.** (Color online) (Left panel) Total density of states for $W_{20}O_{58}$ with idealized crystal structure, (middle panel) density of states for tungsten atoms W1, 12, 14–19, and (right panel) density of states for oxygen atoms in a wide energy range. Zero corresponds to the Fermi level.

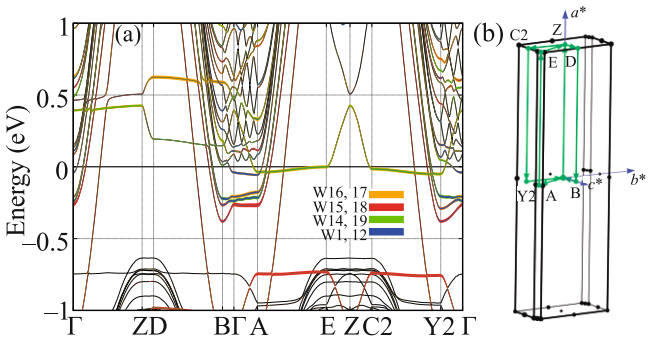


**Fig. 3.** (Color online) (a) Band structure for $W_{20}O_{58}$ with idealized crystal structure near the Fermi level. Color denote the contribution of individual tungsten atoms W1, 12, 14–19. Zero corresponds to the Fermi level. (b) Brillouin zone for idealized crystal structure $W_{20}O_{58}$.

a low-intensity tail coming from W-5*d* states (see Fig. 2), which are filled with electrons due to an oxygen deficit compared to the stoichiometric composition of $WO_3$.

We would like to emphasize the presence of flat bands at the Fermi level in the direction $A$–$E$ and near it, as well as in the direction $\Gamma$–$A$, which are shown in Fig. 3a. For the band structure, we used highly symmetric **k**-points and corresponding directions generated with the SeeK-path tool [38]. They are shown in Fig. 3b.

To demonstrate which states form these flat bands, Fig. 3a shows the band structure with the contributions of individual atoms near the Fermi level. One can see that the flat bands are formed by 5*d*-states of W1, 12, 14–19 tungsten atoms, which are arranged around the voids in zigzag chains of edge-sharing octahedra (see Fig. 1). Located directly around the voids atoms W14, 19 and W16, 17 give the greatest contribution. It is also worth saying that the 5*d* states of W1, 12, 14–19 tungsten provide about 70% to the value of the total state density at the Fermi level. Note that some "chaotic" band structure in the $\Gamma$–$A$ direction, visible above the Fermi level, is nothing but multiple crossing of bands, resulting from the rather small volume of the Brillouin zone and the large number of atoms in the unit cell, split between themselves by small hybridization interaction.

Figure 4 shows the Fermi surface for $W_{20}O_{58}$ with an idealized crystal structure. The corresponding Fermi surface contains six sheets. The sheets located near the $\Gamma$-point (yellow and red) are clearly three-dimensional, while the other sheets are quasi-two-dimensional. Note that the flat bands at the Fermi level in the $A$–$E$ direction form rather large two-dimensional hole pockets at the corners of the Brillouin zone.

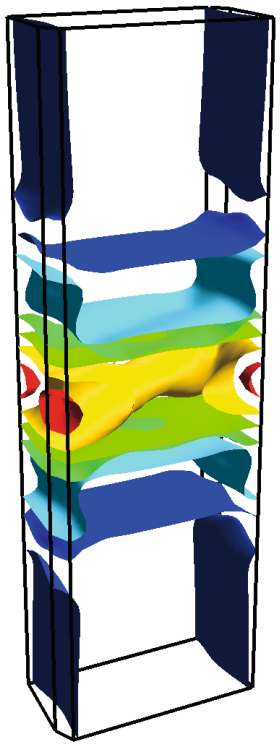

**Fig. 4.** (Color online) Fermi surface for idealized crystal structure $W_{20}O_{58}$.

## 3. CONCLUSIONS

We have studied the compound $W_{20}O_{58}$ with an idealized crystal structure via the ab initio DFT-GGA calculation. Despite the large number of atoms (78) in the unit cell the main contribution to the states near the Fermi level originate from the 5*d*-orbitals of tungsten. These atoms are located directly around the voids in the zigzag pattern of edge-sharing octahedra. Thus, it is this zigzag pattern, disordering the ideal "checkerboard" arrangement of octahedra, are responsible for conductivity and other effects related to the states near the Fermi surface. On the one hand, we are dealing with a complex crystal structure with a huge unit cell, which is caused by the disordered arrangement of some tungsten atoms, and on the other hand, the 5*d*-orbitals of these atoms determine the low-energy physics of the compound $WO_{3-x}$.

## ACKNOWLEDGMENTS

We are grateful to S.G. Ovchinnikov and M.V. Sadovskii for useful discussions. The computations were performed at the URAN supercomputer, Institute of Mathematics and Mechanics, Ural Branch, Russian Academy of Sciences.

## FUNDING

This work was supported by the Russian Foundation for Basic Research, the Government of Krasnoyarsk Territory, and Krasnoyarsk Regional Fund of Science (project no. 19-42-240007 "Electronic Correlation Effects and Multiorbital Physics in Iron-Based Materials and Cuprates," M.M.K.), by the Russian Foundation for Basic Research (project nos. 18-02-00281 and 20-02-00011, I.A.N., N.S.P., A.A.S.), and by the of the President of the Russian Federation for State Support of Young Scientists and Leading Scientific Schools (project no. MK-1683.2019.2, N.S.P. and A.A.S.).

## REFERENCES

1. J. G. Bednorz and K. A. Müller, Zeitschr. Phys. B **64**, 189 (1986).
2. Y. Kamihara, T. Watanabe, M. Hirano, and H. Hosono, J. Am. Chem. Soc. **130**, 3296 (2008).
3. M. V. Sadovskii, Phys. Usp. **51**, 1243 (2008).
4. P. J. Hirschfeld, M. M. Korshunov, and I. I. Mazin, Rep. Prog. Phys. **74**, 124508 (2011).
5. M. M. Korshunov, Phys. Usp. **57**, 813 (2014).
6. L. A. Bursill and B. G. Hyde, J. Solid State Chem. **4**, 430 (1972).
7. W. Sahle and M. Nygren, J. Solid State Chem. **48**, 154 (1983).
8. A. Shengelaya, K. Conder, and K. A. Müller, J. Supercond. Nov. Magn. **33**, 301 (2020).
9. A. Aird and E. K. H. Salje, J. Phys.: Condens. Matter **10**, L377 (1998).
10. Y. Kopelevich, R. R. da Silva, and B. C. Camargo, Phys. C (Amsterdam, Neth.) **514**, 237 (2015).
11. S. Reich and Y. Tsabba, Eur. Phys. J. B **9**, 1 (1999).
12. A. Shengelaya and K. A. Müller, J. Supercond. Nov. Magn. **32**, 3 (2019).
13. H. Hamdi, E. K. H. Salje, Ph. Ghosez, and E. Bousquet, Phys. Rev. B **94**, 245124 (2016).
14. G. A. de Wijs, P. K. de Boer, R. A. de Groot, and G. Kresse, Phys. Rev. B **59**, 2684 (1999).
15. P. P. González-Borrero, F. Sato, A. N. Medina, M. L. Baesso, A. C. Bento, G. Baldissera, C. Persson, G. A. Niklasson, C. G. Granqvist, and A. Ferreira da Silva, Appl. Phys. Lett. **96**, 061909 (2010).
16. M. B. Johansson, G. Baldissera, I. Valyukh, C. Persson, H. Arwin, G. A. Niklasson, and L. Österlund, J. Phys.: Condens. Matter **25**, 205502 (2013).
17. Y. Ping, D. Rocca, and G. Galli, Phys. Rev. B **87**, 165203 (2013).
18. A. C. Tsipis and C. A. Tsipis, J. Phys. Chem. A **104**, 859 (2000).
19. M. G. Stachiotti, F. Cor'a, C. R. A. Catlow, and C. O. Rodriguez, Phys. Rev. B **55**, 7508 (1997).
20. F. Corà, A. Patel, N. M. Harrison, R. Dovesi, and C. R. A. Catlow, J. Am. Chem. Soc. **118**, 12174 (1996).
21. D. B. Migas, V. L. Shaposhnikov, V. N. Rodin, and V. E. Borisenko, J. Appl. Phys. **108**, 093713 (2010).
22. F. Wang, C. di Valentin, and G. Pacchioni, J. Phys. Chem. C **115**, 8345 (2011).
23. F. Wang, C. di Valentin, and G. Pacchioni, Phys. Rev. B **84**, 073103 (2011).
24. S. Zh. Karazhanov, Y. Zhang, A. Mascarenhas, S. Deb, and W. Wang, Solid State Ion **165**, 43 (2003).
25. F. Mehmood, R. Pachter, N. R. Murphy, W. E. Johnson, and Ch. V. Ramana, J. Appl. Phys. **120**, 233105 (2016).
26. A. D. Walkingshaw, N. A. Spaldin, and E. Artacho, Phys. Rev. B **70**, 165110 (2004).
27. S. Tosoni, C. di Valentin, and G. Pacchioni, J. Phys. Chem. C **118**, 3000 (2014).
28. A. Hjelm, C. G. Granqvist, and J. M. Wills, Phys. Rev. B **54**, 2436 (1996).
29. B. Ingham, S. C. Hendy, S. V. Chong, and J. L. Tallon, Phys. Rev. B **72**, 075109 (2005).
30. M. N. Huda, Y. Yan, S.-H. Wei, M. M. Al-Jassim, Phys. Rev. B **80**, 115118 (2009).
31. F. Corà, M. G. Stachiotti, C. R. A. Catlow, and C. O. Rodriguez, J. Phys. Chem. **101**, 3945 (1997).
32. M. N. Huda, Y. Yan, Ch.-Y. Moon, S.-H. Wei, and M. M. Al-Jassim, Phys. Rev. B **77**, 195102 (2008).
33. B. Chen, J. Laverock, L. F. J. Piper, A. R. H. Preston, S. W. Cho, A. DeMasi, K. E. Smith, D. O. Scanlon, G. W. Watson, R. G. Egdell, P.-A. Glans, and J.-H. Guo, J. Phys.: Condens. Matter **25**, 165501 (2013).
34. D. B. Migas, V. L. Shaposhnikov, and V. E. Borisenko, J. Appl. Phys. **108**, 093714 (2010).
35. A. Magnéli, Arkiv Kemi **1**, 513 (1949).
36. J. P. Perdew, K. Burke, and M. Ernzerhof, Phys. Rev. Lett. **77**, 3865 (1996).
37. The Elk Code. http://elk.sourceforge.net/.
38. Y. Hinuma, G. Pizzi, Y. Kumagai, F. Oba, and I. Tanaka, Comput. Mater. Sci. **128**, 140 (2017).

*Translated by the author*